Chapter 22
Allocation and Sizing of Multiple Tuned Mass Dampers for Seismic Control of Irregular Structures

Yael Daniel and Oren Lavan

Abstract This chapter presents a methodology for the optimal design of multiple tuned mass dampers (TMDs) in 3D irregular buildings. The objective function minimizes the total mass of all added TMDs while constraints are added to limit the total accelerations experienced at the edges of the floors in the direction parallel to each edge. The formulation of the design methodology relies on optimality criteria conjectured herein; hence, a two-stage iterative analysis/redesign procedure, that is based on analysis tools only, is resulted. The methodology applies to all types of irregularity, which allows the application of the methodology in a practical design process.

22.1 Introduction

Seismic protection of structures is an important issue in structural design due to its threatening consequences. Often, it is required that the design of the structure provide even more than life safety, promising a certain level of serviceability following a severe earthquake, while allowing for a defined level of damage, i.e., performance-based design. In performance-based design, it is often desired to limit important responses such as inter-story drifts, total accelerations, residual drifts, and hysteretic energy.

There is ample literature on the reduction of structural responses to earthquakes through passive control. Several passive damping devices are available, including viscous, viscoelastic, metallic, and friction dampers (see, e.g., Soong and Dargush 1997; Christopoulos and Filiatrault 2006; Takewaki 2009). For wind vibration

Y. Daniel (✉) • O. Lavan
Faculty of Civil and Environmental Engineering, Technion – Israel Institute of Technology, Haifa 32000, Israel
e-mail: yaeldan@tx.technion.ac.il; lavan@tx.technion.ac.il

O. Lavan and M. De Stefano (eds.), *Seismic Behaviour and Design of Irregular and Complex Civil Structures*, Geotechnical, Geological and Earthquake Engineering 24, DOI 10.1007/978-94-007-5377-8_22,

control of tall buildings, tuned mass dampers (TMDs) are often effectively used (e.g., McNamara 1977). Details about TMDs and their applications may be found in the fine works of Den-Hartog (1940), Warburton (1982), and Soong and Dargush (1997), only to name a few. As wind response of buildings is kept within the linear range and is usually dominated by a single mode, TMDs indeed provide a very efficient solution. Seismic action, on the other hand, may cause yielding of the structure, which can jeopardize the action of TMDs due to their detuning. In addition, in seismic vibrations, no single distinct frequency dominates the behavior, but rather many frequencies, including the ones of higher modes. Those two obstacles have led many researchers to be hesitant in using TMDs for seismic structural applications (e.g., Kaynia et al. 1981; Sladek and Klingner 1983). Nonetheless, provided those obstacles are overcome, TMDs could provide a very promising alternative for multi-hazard mitigation for both winds and earthquakes.

The two aforementioned obstacles can often be overcome quite easily. In some cases where TMDs are used, inter-story drifts may already be reduced below yield drifts, and thus the structure remains elastic. A particular example to that could be found in cases where the static portion of wind loading dominates the lateral load design which results in a stiff and strong structure. Here, of course, the reduction of other structural responses (e.g., total accelerations) to both winds and earthquakes may also be desired. In addition, even if yielding does occur, causing the effective structure's stiffness to shift and thus the TMD to detune, the use of a semi-active TMD (SATMD) has been proposed (e.g., Nagarajaiah and Sonmez 2007; Roffel et al. 2010). Another approach that is based on passive control could split the TMD to several TMDs, each tuned to a slightly different frequency within a bandwidth close to the natural frequency of the main system, thus reducing the detuning effect and allowing design robustness (e.g., Xu and Igusa 1992), and in the case of 3D structures, (Jangid and Datta 1997; Li and Qu 2006). Of course, this approach is suitable only for cases where yielding is limited.

As for the second obstacle, regarding the multimodal seismic response, several solutions were proposed. One solution is the use of an active TMD (ATMD) which uses a control law to alter the frequency of the device at each moment (e.g., Abdel-Rohman 1984). This solution, however, requires a large external power supply to be activated, which may be costly and may force a reliability issue during an actual earthquake. Another possible solution, that is adopted herein, is the use of multiple TMDs (MTMDs), each tuned to a different frequency. These MTMDs could be distributed along the structure and located at locations which will optimize the control of the structure. The idea of using MTMDs tuned to various natural frequencies of the structure is not new. Clark (1988) indicated that a single TMD cannot significantly reduce the motion created due to seismic excitations, while MTMDs can substantially reduce motion. Moon (2010) shows a practical application of vertically distributed MTMDs in tall buildings for reducing wind-induced vibrations and offers a method of distributing them by mode shape.

In the literature, there are not many methodologies available for the design of MTMDs of various frequencies and locations in seismic application. In their pioneering work, Chen and Wu (2001) use a frequency-based transfer function as a response measure of the multimodal vibration problem of structures and allocate multimodal MTMDs using a sequential search technique. Luo et al. (2009) minimized a dynamic magnification factor of the first mode obtained based on the transfer function of the structure's response in frequency domain. Lin et al. (2010) proposed a two-stage frequency domain-based optimal design of MTMDs taking into consideration both the structural response and the TMD stroke. Fu and Johnson (2011) suggest using passive MTMDs with a vertical distribution of mass, where each story is assigned with one TMD of which its parameters are optimized as to minimize the sum of inter-story drifts. As for methodologies for designing 3D asymmetric structures, several methodologies using genetic algorithms exist (Singh et al. 2002; Ahlawat and Ramaswamy 2003; Desu et al. 2007). Other optimization methods for similar problems were taken in (Lin et al. 1999, 2011). Some of these methodologies only allow for dampers to dampen a single mode. While the above methodologies present a huge step forward, there is still no methodology which allows the possible dampening of all modes and leads to a desired performance in small computational efforts while using analysis tools only.

This chapter presents a simple performance-based design methodology for the allocation and sizing problem of multimodal MTMDs in structures undergoing seismic excitations. In many cases where TMDs are considered for wind mitigation, the static portion of wind loading dominates the lateral load design to result a stiff and strong structure. Hence, with the addition of TMDs, inter-story drifts may not be the main response of concern, and the reduction of total accelerations may become of major importance. Hence, the objective function minimizes the total mass of all added TMDs, while limiting the total accelerations experienced at the edges of the floors in the direction parallel to each edge. The methodology is based on a simple iterative analysis/redesign procedure where, first, an analysis is performed for a given design and then redesign of the TMDs is performed according to recurrence relations. The redesign first determines the mass of all dampers at a given location based on local acceleration measures. It is then distributed between dampers tuned to various frequencies. The proposed performance-based methodology is simple, relies on analyses tools only, generally applies to any irregular 3D problem, and possesses fast convergence.

22.2 Problem Formulation

22.2.1 Equations of Motion

Following Soong and Dargush (1997), the equations of motion of a MDOF system can be represented in state-space notation as

$$\dot{\hat{\mathbf{x}}}(t) = \mathbf{A} \cdot \hat{\mathbf{x}}(t) + \mathbf{B} \cdot a_g(t); \quad \mathbf{y}(t) = \mathbf{CC} \cdot \hat{\mathbf{x}}(t) \tag{22.1}$$

where $\hat{\mathbf{x}}^{\mathrm{T}} = \left[\mathbf{x}^{\mathrm{T}}\ \dot{\mathbf{x}}^{\mathrm{T}}\right]$; $\mathbf{x} \in R^N$, $\hat{\mathbf{x}} \in R^{2N}$ is the state variable vector, $\mathbf{x}(t)$ is the displacement vector between the DOFs and the ground, $a_g(t)$ is the ground motion's acceleration, a dot represents the derivative with respect to time, and $\mathbf{y}(t)$ is the output vector of the system, whose entries are responses of interest. Those responses are a linear combination of the state variables and the input forces (in our case $\mathbf{y}(t) = \mathbf{x}(t)$ gives an output of displacements, absolute acceleration will be accounted for later). The matrices **A**, **B**, and **CC** are defined as following

$$\mathbf{A} = \begin{bmatrix} \mathbf{0}_{N\times N} & \mathbf{I}_{N\times N} \\ -\mathbf{M}^{-1}\mathbf{K} & -\mathbf{M}^{-1}\mathbf{C} \end{bmatrix} \quad \mathbf{B} = \begin{bmatrix} \mathbf{0}_{N\times 1} \\ -\mathbf{e} \end{bmatrix} \quad \mathbf{CC} = \begin{bmatrix} \mathbf{I}_{N\times N} & \mathbf{0}_{N\times N} \end{bmatrix} \tag{22.2}$$

where **M**, **C**, and **K** are the mass, inherent damping, and stiffness matrices of the structure according to the chosen N degrees of freedom (DOFs), respectively, **e** is the excitation direction vector, **I** is the identity matrix, and **0** is a zero matrix of appropriate dimensions as noted. It should be noted that for the sake of presentation, Eq. (22.1) and the following methodology are presented using a single input (component of the ground motion).

22.2.2 Performance Measures

As previously mentioned, there are many cases where inter-story drifts and structural damage levels under a severe ground motion obtain acceptable values. In these situations, total accelerations are to be limited.

Added TMDs help control the responses of the structure, and the measure of cost of this controlling system is by the amount of added mass. As more mass is added to the structure, the retrofit is said to be more expensive and thus less cost-effective.

22.2.3 Problem Formulation

This work makes use of a stochastic description of the ground motion. The problem is formulated as an optimization problem for which the objective function minimizes the total amount of added masses in the TMDs under constraints of maximal performance measures. The design variables are the mass of each TMD, located in parallel to the edges of all floors. The root-mean-square (RMS) total accelerations at all peripheral locations of all floors are taken as the performance measures, as they are the largest accelerations expected within story limits. Those locations are shown in Fig. 22.1 as $(\mathbf{x}_{\mathrm{pyl}})_n$, $(\mathbf{x}_{\mathrm{pyr}})_n$, $(\mathbf{x}_{\mathrm{pxt}})_n$, and $(\mathbf{x}_{\mathrm{pxb}})_n$ and are the peripheral coordinates in the "y," "y," "x," and "x" directions at the left, right, top, and bottom edges of floor n, respectively. The remaining variables in Fig. 22.1 will be explained subsequently. That is, the constraints are on the total accelerations at the edges of all floors in the directions parallel to each edge. The optimization problem is thus formulated as

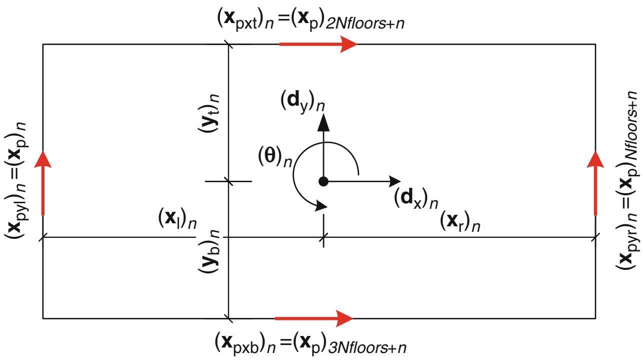

Fig. 22.1 Definition of dynamic DOFs and peripheral coordinates of the *n*th floor

$$\min_{(\mathbf{m}_{\text{TMD}})_{l,f}} J = \sum_{l}^{\substack{\text{all}\\ \text{locations}}} \sum_{f}^{\substack{\text{all}\\ \text{frequencies}}} (\mathbf{m}_{\text{TMD}})_{l,f}$$

$$\text{s.t.} \quad \frac{\text{RMS}\left(\left(\ddot{\mathbf{x}}_{\text{p}}^{\text{t}}\right)_l\right)}{a_{\text{all}}^{\text{RMS}}} \le 1.0 \quad \forall l = 1, 2, \ldots, N_{\text{locations}} \tag{22.3}$$

where $(\mathbf{m}_{\text{TMD}})_{l,f}$ is the mass of the TMD located at peripheral location l tuned to frequency f, $N_{\text{locations}}$ is the number of locations to be dampened, $a_{\text{all}}^{\text{RMS}}$ is the allowable RMS total acceleration, and $\text{RMS}\left(\left(\ddot{\mathbf{x}}_{\text{p}}^{\text{t}}\right)_l\right)$ is the root mean square of the total acceleration at location l (the lth term of $\text{RMS}\left(\ddot{\mathbf{x}}_{\text{p}}^{\text{t}}\right)$). Such reference to a component of a vector or a matrix, i.e., $(\cdot)_l$, will be used throughout the chapter.

22.3 Proposed Solution Scheme

22.3.1 Fully Stressed Design

Designs that are based on fully stressed characteristics go back to the classical design of trusses under static loads, whereby the weight is minimized for a given allowable stress. For that problem, it had been widely accepted that the optimal design yields a *statically determinate fully stressed design*, *with members out of the design having strains smaller than the allowable*. This result appeared in the literature as early as 1900 (Cilley 1900). This has been proven in several occasions, using various approaches (Cilley 1900; Mitchell 1904; Levy 1985).

Recently, it was shown that some dynamic optimal designs also possess “fully stressed” characteristics. Lavan and Levy (2005); Levy and Lavan (2006) considered

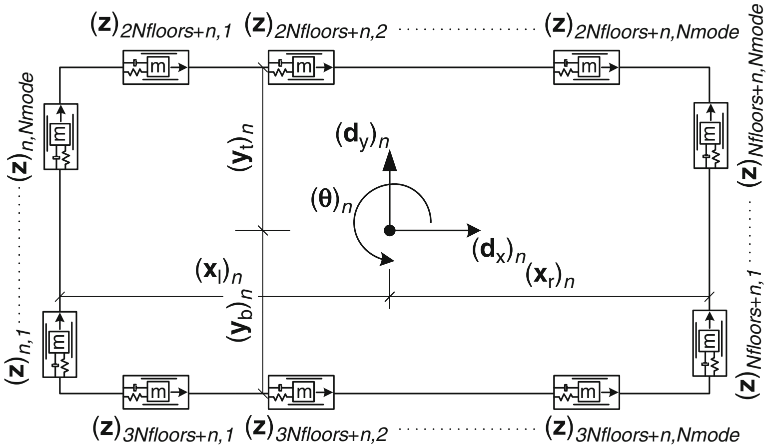

Fig. 22.2 Locations of TMDs at the floor n and their associated z DOFs

the minimization of total added viscous damping to frame structures subjected to ground accelerations while constraining various inter-story responses. Their optimal solutions attained by formal optimization indicated that "At the optimum, damping is assigned to stories for which the local performance index has reached the allowable value. Stories with no assigned damping attain a local performance index which is lower or equal to the allowable." That is, the optimal solutions attained "fully stressed" characteristics.

Based on past experience of the authors in similar problems, it is conjectured here that the optimal solution to MTMD allocation and sizing in structures under a stochastic ground acceleration input (solution of Eq. (22.3)) possesses fully stressed design (FSD) characteristics, i.e., "At the optimum, TMDs are assigned to peripheral locations for which the RMS total acceleration has reached the allowable value under the considered input acceleration PSD. In addition, at each location to which TMDs are added, TMDs of a given frequency are assigned only to frequencies for which the output spectral density is maximal."

Potential locations for TMDs are located at the edges of the floors, as their lines of action are in direction parallel to the edges (Fig. 22.2). Those are actually the same locations where total accelerations are to be limited.

Stage one of the conjecture imposes that for all peripheral locations with masses within the design, the total acceleration equals the allowable one, while all peripheral locations with zero masses (outside the design) have an acceleration equal to or less than the allowable. This is illustrated on the left-hand side of Fig. 22.3, which presents the concept on a selected peripheral frame. The second stage of the conjecture imposes that for all dampers at a peripheral location where the acceleration equals the allowable one, and are within the design, the output spectral densities are maximal (with respect to ω) and equal. As for masses outside

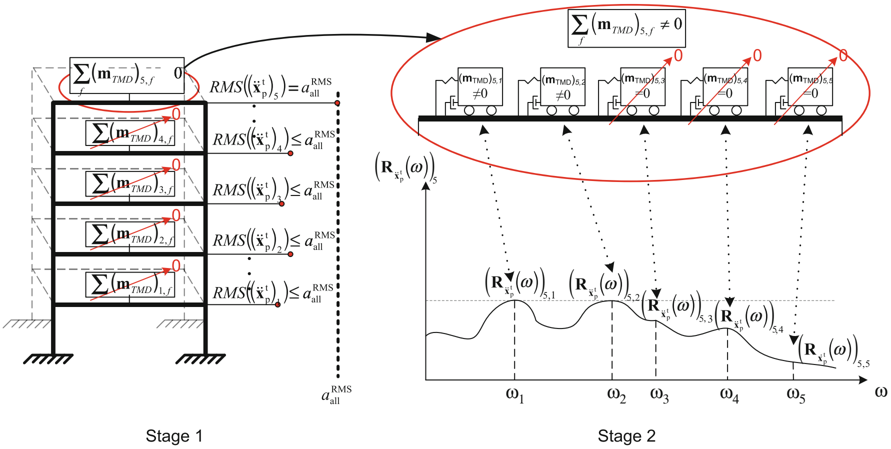

Fig. 22.3 Illustrations of conjecture

of the design at this DOF, the output spectral density is less than maximal. This is illustrated on the right-hand side of Fig. 22.3.

The above conjecture suggests that the tuning frequency of each TMD is searched for among all possible frequencies. However, for practical reasons, it is reasonable to assume that these frequencies are in the vicinity of the bare structure's frequencies, and thus the tuning of TMDs could be in relation to the bare structure's natural frequency.

22.3.2 Analysis/Redesign Algorithm

Solutions to optimization problems, which possess fully stressed characteristics, are efficiently achieved iteratively using a two-step algorithm in each iteration cycle. In the first step, an analysis is performed for a given preliminary design, whereas in the second step, the design is changed using a recurrence relationship that targets fully stressedness. The recurrence relation can be generally written as

$$x_l^{(n+1)} = x_l^{(n)} \cdot \left(\frac{pi_l^{(n)}}{pi_{\text{allowable}}} \right)^P \tag{22.4}$$

where x_l is the value of the design variable associated with the location l, pi_l is the performance measure of interest for the location l, $pi_{\text{allowable}}$ is the allowable value for the performance measure, n is the iteration number, and P is a convergence parameter. Fully stressedness is obtained from using Eq. (22.4) since upon convergence, one of the following must take place. Either $x_l^{(n+1)} = x_l^{(n)}$ giving $pi_l^{(n)} = pi_{\text{allowable}}$ or $x_l^{(n+1)} = x_l^{(n)} = 0$ giving $pi_l^{(n)} \le pi_{\text{allowable}}$.

The advantages of the analysis/redesign algorithm include its simplicity, the need to use analysis tools only, and the fairly small computational effort that lies in the small number of analyses required for convergence. Such analysis/redesign procedure will be utilized here to attain fully stressed designs where the mass, frequency, and locations of MTMDs within framed structures are to be determined.

22.3.3 Proposed Solution Scheme

The proposed design methodology relies on the analysis/redesign procedure which leads to the FSD criteria presented above:

Step 1: An allowable RMS acceleration is chosen. The mass, damping, and stiffness matrices of the structure are assembled.

Step 2: Solution of the eigenvalue problem determines the structure's natural frequencies and mode shapes.

Step 3: A power spectral density (PSD) for the input acceleration is chosen. Examples of such input spectra are stationary white noise, which gives a constant PSD, and the Kanai-Tajimi (1957) PSD. The PSD is fitted to represent real ground motions. This is done by fitting its parameters to a frequency-based spectrum representing the decomposition of earthquakes into frequency components (e.g., a FFT spectrum). For each DOF, the transfer function of total acceleration of the bare frame is evaluated using Eq. (22.5). This transfer function represents the ratio between the sinusoidal output amplitude and the sinusoidal input amplitude with frequency ω. For total accelerations, it can be shown that the appropriate transfer vector, $\mathbf{H}_{\ddot{\mathbf{x}}^{\mathrm{t}}}(j\omega)$, is

$$\mathbf{H}_{\ddot{\mathbf{x}}^{\mathrm{t}}}(j\omega) = -\mathbf{M}^{-1} \cdot (j\omega\mathbf{C} + \mathbf{K}) \cdot \mathbf{H}_{\mathbf{x}}(j\omega) \tag{22.5}$$

where $j = \sqrt{-1}$ and $\mathbf{H}_{\mathbf{x}}(j\omega)$ is the displacement transfer vector given by (Kwakernaak and Sivan 1991)

$$\mathbf{H}_{\mathbf{x}}(j\omega) = \mathbf{CC} \cdot (j\omega\mathbf{I} - \mathbf{A})^{-1} \cdot \mathbf{B} \tag{22.6}$$

This transfer function is transformed to peripheral coordinates using

$$\mathbf{H}_{\ddot{\mathbf{x}}_{\mathrm{p}}^{\mathrm{t}}}(j\omega) = \mathbf{T} \cdot \mathbf{H}_{\ddot{\mathbf{x}}^{\mathrm{t}}}(j\omega) \tag{22.7}$$

where $\mathbf{H}_{\ddot{\mathbf{x}}_{\mathrm{p}}^{\mathrm{t}}}(j\omega)$ is the structure's transfer function of total accelerations in peripheral coordinates and $\mathbf{T}$ is a transformation matrix from the original DOFs to peripheral coordinates. The output spectral densities of the peripheral accelerations, $\left(\mathbf{R}_{\ddot{\mathbf{x}}_{\mathrm{p}}^{\mathrm{t}}}(\omega)\right)_l$, are evaluated using

$$\left(\mathbf{R}_{\ddot{\mathbf{x}}_{\mathrm{p}}^{\mathrm{t}}}(\omega)\right)_{l}=\left|\left(\mathbf{H}_{\ddot{\mathbf{x}}_{\mathrm{p}}^{\mathrm{t}}}(j\omega)\right)_{l}\right|^{2}\cdot S(\omega) \tag{22.8}$$

where $S(\omega)$ is the input PSD, $\left|\left(\mathbf{H}_{\ddot{\mathbf{x}}_{\mathrm{p}}^{\mathrm{t}}}(j\omega)\right)_{l}\right|^{2}=\left(\mathbf{H}_{\ddot{\mathbf{x}}_{\mathrm{p}}^{\mathrm{t}}}(j\omega)\right)_{l}\cdot\left(\mathbf{H}^{*}_{\ddot{\mathbf{x}}_{\mathrm{p}}^{\mathrm{t}}}(j\omega)\right)_{l}$, $(\mathbf{H}_{\ddot{\mathbf{x}}^{\mathrm{t}}}(j\omega))_{l}$ is the lth term of $\mathbf{H}_{\ddot{\mathbf{x}}^{\mathrm{t}}}(j\omega)$, and $\left(\mathbf{H}^{*}_{\ddot{\mathbf{x}}^{\mathrm{t}}}(j\omega)\right)_{l}$ is its complex conjugate.

The area under the output spectral density curve equals the mean-square response (Newland 1993), and, thus, the root mean square (RMS) of total accelerations at peripheral coordinate l, $\mathrm{RMS}\left(\ddot{\mathbf{x}}_{\mathrm{p}}^{\mathrm{t}}\right)_{l}$,taking into consideration the contribution of all frequencies to the total response, is derived using

$$\mathrm{RMS}\left(\ddot{\mathbf{x}}_{\mathrm{p}}^{\mathrm{t}}\right)_{l}=\sqrt{2\cdot\int_{0}^{\infty}\left(\mathbf{R}_{\ddot{\mathbf{x}}_{\mathrm{p}}^{\mathrm{t}}}(\omega)\right)_{l}\mathrm{d}\omega} \tag{22.9}$$

Step 4: If for any peripheral coordinate, l, the RMS acceleration obtained is larger than the allowable RMS acceleration, MTMDs are added to suppress the acceleration produced. Each TMD of mass $(\mathbf{m}_{\mathrm{TMD}})_{l,f}$ is assigned with a DOF for its displacement relative to the ground, $(\mathbf{z})_{l,f}$. Here, the subscript l stands for its location while the subscript f stands for its frequency. The location, l, is corresponding to the peripheral coordinate $(\mathbf{x}_{\mathrm{p}})_{l}$ the TMD is attached to. At each location, N_{mode} TMDs are added, to suppress N_{mode} original frequencies of the structure, where N_{mode} is the number of modes to potentially be controlled. Thus, generally, a total of $N_{\mathrm{mode}}\cdot N_{\mathrm{locations}}$ dampers are potentially added (Fig. 22.2).

The response of each mode could be evaluated based on a single-degree-of-freedom (SDOF) equivalent system. Hence, properties of the TMDs to dampen a certain mode could be set based on its SDOF representation. For the sake of simplicity in this chapter, Den-Hartog's (1940) properties were chosen. Nonetheless, more advanced criteria could easily be used with the proposed methodology. These Den-Hartog properties were derived for the optimal reduction of mass displacement of an SDOF system under external sinusoidal loading. They were later shown to also reduce the maximum total acceleration response of the mass of an SDOF system undergoing a harmonic base excitation (Warburton 1982). In the case of optimal Den-Hartog properties, the following initial properties are taken for the dampers:

1. The initial mass of all TMDs located at each peripheral coordinate is taken as certain predetermined percentage of the structure's mass (say 1%) and divided equally between the TMDs

$$(\mathbf{m}_{\mathrm{TMD}})_{l,f}=\left(\frac{0.01\cdot M_{\mathrm{structure}}}{N_{\mathrm{mode}}}\right) \tag{22.10}$$

where l represents the damper's location, f represents the mode dampened, and $M_{\mathrm{structure}}$ is the structure's total mass. The mass ratio $(\mu_{\mathrm{TMD}})_{f}$ of all TMDs tuned to frequency f is calculated as the ratio between the effective TMD mass of all

TMDs tuned to frequency f and the fth modal mass of the structure. This mass ratio is defined as

$$(\boldsymbol{\mu}_{\text{TMD}})_f = \frac{\left(\varphi_f^{\text{T}} \cdot \mathbf{T}^{\text{T}} \cdot D\left((\mathbf{m}_{\text{TMD}})_f\right) \cdot \mathbf{T} \cdot \varphi_f\right)}{\left(\varphi_f^{\text{T}} \cdot \mathbf{M}_{\mathbf{original}} \cdot \varphi_f\right)} \tag{22.11}$$

where φ_f is the fth mode shape of the bare structure, $\left[\mathbf{M}_{\mathbf{original}}\right]$ is the bare frame's mass matrix, and $D\left((\mathbf{m}_{\text{TMD}})_f\right)$ is a diagonal matrix with the terms $(\mathbf{m}_{\text{TMD}})_{1:N_{\text{locations}},f}$ sitting on the diagonal.

2. Each TMD's stiffness is determined according to the frequency of the mode which is dampened by the TMD and is tuned to

$$(\boldsymbol{\omega}_{\text{TMD}})_f = \frac{(\boldsymbol{\omega}_{\text{n}})_f}{\left(1 + (\boldsymbol{\mu}_{\text{TMD}})_f\right)} \tag{22.12}$$

where $(\boldsymbol{\omega}_{\text{n}})_f$ is the frequency f to be dampened. The compatible stiffness is

$$(\mathbf{k}_{\text{TMD}})_{l,f} = (\mathbf{m}_{\text{TMD}})_{l,f} \cdot \left((\boldsymbol{\omega}_{\text{TMD}})_f\right)^2 \tag{22.13}$$

3. Each TMD's modal damping ratio is determined according to

$$(\boldsymbol{\xi}_{\text{TMD}})_f = \sqrt{\frac{3 \cdot (\boldsymbol{\mu}_{\text{TMD}})_f}{\left(8 \cdot \left(1 + (\boldsymbol{\mu}_{\text{TMD}})_f\right)^3\right)}} \tag{22.14}$$

and the matching damping coefficient

$$(\mathbf{c}_{\text{TMD}})_{l,f} = 2 \cdot (\mathbf{m}_{\text{TMD}})_{l,f} \cdot (\boldsymbol{\xi}_{\text{TMD}})_f \cdot (\boldsymbol{\omega}_{\text{n}})_f \tag{22.15}$$

Step 5: The mass, damping, and stiffness matrices of the damped frame are formulated. Note the mass of TMDs is to be added to the mass of the structure perpendicular to their original DOF (i.e., if a certain damper is used to reduce vibration in the "y" direction and thus its DOF is in the "y" direction, the mass of that TMD is added to the mass of the structure in the "x" direction of the story where it is situated).

Step 6: The peripheral RMS accelerations of the damped frame at all coordinates are evaluated using frequency domain analysis based on Eqs. (22.5), (22.6), (22.7), (22.8), and (22.9), using the newly updated matrices (note that in Eq. (22.9), it is needed to take only the first N components of the extended vector $\mathbf{H}_{\ddot{\mathbf{x}}^{t}}(j\omega)$ as now DOFs of TMDs are included in this vector).

Step 7: The TMD's mass is redetermined using two stages; the total mass of all dampers located at a given location is determined, followed by the distribution of that mass between all TMDs at that location, having various tuning frequencies. This is done according to the recurrence relationships described below. Following the change in mass, the stiffness and modal damping ratios of each TMD are also updated while keeping the Den-Hartog principles intact, using Eqs. (22.11), (22.12), (22.13), (22.14), and (22.15). The two-stage analysis/redesign procedure is carried out iteratively in the following way

Stage 1:

$$\left(\mathbf{m}_{\mathrm{TMD,total}}^{(n+1)}\right)_l = \sum_{f=1}^{\substack{\text{all}\\ \text{frequencies}}} \left(\mathbf{m}_{\mathrm{TMD}}^{(n+1)}\right)_{l,f} = \sum_{f=1}^{\substack{\text{all}\\ \text{frequencies}}} \left(\mathbf{m}_{\mathrm{TMD}}^{(n)}\right)_{l,f} \cdot \left(\frac{\mathrm{RMS}\left(\left(\ddot{\mathbf{x}}_{\mathrm{p}}^{\mathrm{t}\,(n)}\right)_l\right)}{a_{\mathrm{all}}^{\mathrm{RMS}}}\right)^P \tag{22.16}$$

where $(\cdot)^{(n)}$ is the value at iteration n, $\left(\mathbf{m}_{\mathrm{TMD,total}}^{(n+1)}\right)_l$ is the total mass of all dampers at location l, and P is a constant which influences the convergence and convergence rate. A large P will result in a faster but less stable convergence of the above equation.

Stage 2:

$$\left(\mathbf{m}_{\mathrm{TMD}}^{(n+1)}\right)_{l,f} = \left(\mathbf{m}_{\mathrm{TMD}}^{(n)}\right)_{l,f} \left(\frac{\sqrt{\left(\mathbf{R}_{\ddot{\mathbf{x}}_{\mathrm{p}}^{\mathrm{t}}}^{(n)}\left((\omega_{\mathrm{n}})_f\right)\right)_l}}{\max\limits_f\left(\sqrt{\left(\mathbf{R}_{\ddot{\mathbf{x}}_{\mathrm{p}}^{\mathrm{t}}}^{(n)}\left((\omega_{\mathrm{n}})_f\right)\right)_l}\right)}\right)^P \cdot \frac{\left(\mathbf{m}_{\mathrm{TMD,total}}^{(n+1)}\right)_l}{\sum\limits_{f=1}^{\substack{\text{all}\\ \text{frequencies}}} \left(\mathbf{m}_{\mathrm{TMD}}^{(n)}\right)_{l,f} \left(\frac{\sqrt{\left(\mathbf{R}_{\ddot{\mathbf{x}}_{\mathrm{p}}^{\mathrm{t}}}^{(n)}\left((\omega_{\mathrm{n}})_f\right)\right)_l}}{\max\limits_f\left(\sqrt{\left(\mathbf{R}_{\ddot{\mathbf{x}}_{\mathrm{p}}^{\mathrm{t}}}^{(n)}\left((\omega_{\mathrm{n}})_f\right)\right)_l}\right)}\right)^P} \tag{22.17}$$

where $\left(\mathbf{R}_{\ddot{\mathbf{x}}_{\mathrm{p}}^{\mathrm{t}}}^{(n)}\left((\omega_{\mathrm{n}})_f\right)\right)_l$ is the component of $\mathbf{R}_{\ddot{\mathbf{x}}_{\mathrm{p}}^{\mathrm{t}}}^{(n)}(\omega)$ at the location l evaluated at $\omega = (\omega_{\mathrm{n}})_f$.

Step 8: Repeat steps 5–7 until convergence of the mass is reached.

22.4 Example

The following 8-story setback RC frame structure (Fig. 22.4) introduced by Tso and Yao (1994) is retrofitted using MTMDs for ground motions exciting the structure in the "y" direction. A uniform distributed mass of 0.75 ton/m^2 is taken. The column dimensions are 0.5 m by 0.5 m for frames 1 and 2 and 0.7 m by 0.7 m for frames 3 and 4. The beams are 0.4 m wide and 0.6 m tall. Five percent Rayleigh damping for the first and second modes is used. A 45% reduction of the RMS total acceleration in the bare structure is desired. Hence, an allowable peripheral RMS acceleration of 55% of the maximal peripheral RMS acceleration of the bare structure is adopted. The response is analyzed under a Kanai-Tajimi PSD with parameters fitted to the average FFT values of the SE 10 in 50 ground motion ensemble (Somerville et al. 1997). The design variables are the locations and properties of the individual tuned mass dampers. The dampers are to potentially be located in the peripheral frames, where they are most effective, and as the excitation is in the "y" direction only, dampers will be assigned only to the peripheral frames 1 (lower 4 floors), 3 (upper 4 floors), and 4 to dampen frequencies of modes which involve "y" and "θ." The steps described above are closely followed to optimally design the MTMDs.

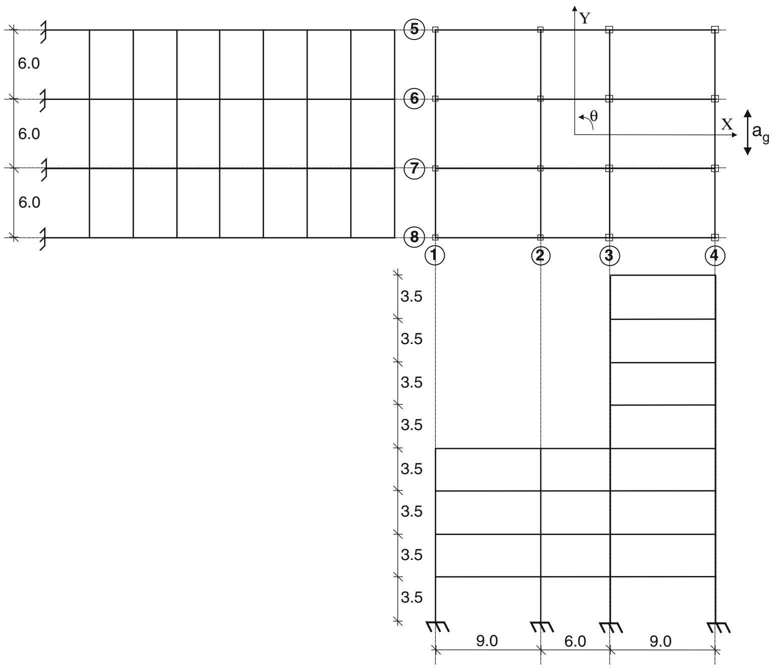

Fig. 22.4 Eight-story setback structure

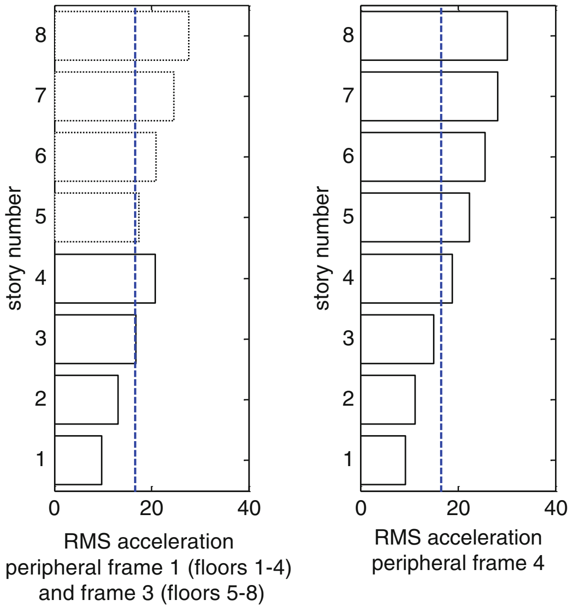

Fig. 22.5 Peripheral RMS accelerations of bare structure (*continuous* or *dotted*) and allowable values (*dotted*)

Step 1: The mass, inherent damping, and stiffness matrices of the frame were constructed.

Step 2: The natural frequencies of the structure were determined. The first few frequencies are (rad/s): 6.88 (x), 7.36 (y,θ), 10.37 (y,θ), 16.04 (x), 17.88 (y,θ), 22.61 (y,θ), 33.87 (x), 35.96 (y θ), and 43.48 (y,θ) where x,y and θ relate to the mode direction.

Step 3: The RMS accelerations of the undamped building at the peripheral frames in the y direction are presented in Fig. 22.5. Those were obtained using the Kanai-Tajimi PSD with parameters $\omega_g = 13$ rad/s, $\xi_g = 0.98$, and $S_0 = 1$. Those were determined by fitting the parameters ω_g and ξ_g to a spectrum of mean FFT values of the SE 10 in 50 ground motion ensemble scaled to $S_0 = 1.0$. The actual value of S_0 has no effect since the allowable RMS acceleration is determined by the percentage of reduction desired. The allowable RMS acceleration for all peripheral accelerations was earlier adopted as 55% of the maximum peripheral RMS acceleration of the bare frame, giving $a_{\mathrm{all}}^{\mathrm{RMS}} = 16.61$.

Step 4: 160 TMDs were added, as a first guess. Those are comprised of ten dampers each tuned to a different mode frequency (of modes related to "y" and "θ") at each of the 16 peripheral locations of frames 1, upper four floors of frame 3, and frame 4. The initial properties were a mass of 1.782 ton for each TMD; a frequency of (rad/s) 7.18, 10.20, 17.57, 22.15, 35.42, 42.48, 53.36, 65.92, 70.90, and 92.57 (TMDs tuned to dampen modes 2, 3, 5, 6, 8, 9, 11, 12, 13, and 15, respectively); and a damping ratio of 0.0931, 0.0778, 0.0802, 0.0860, 0.0739, 0.0909, 0.0811, 0.0851, 0.0728, and 0.0889. These are based on the Den-Hartog properties of Eqs. (22.11), (22.12), (22.13), (22.14), and (22.15).

Step 5: The mass, stiffness, and damping matrices were updated.

Step 6: With the newly updated matrices and the same PSD input, new peripheral RMS accelerations were evaluated using Eqs. (22.5), (22.6), (22.7), (22.8), and (22.9). Peripheral accelerations smaller than the allowable were attained for all floors of frames 5 and 8 in the x direction (see Fig. 22.4 for frame numbering).

Step 7: The problem has not converged, and thus the TMDs' properties were altered, using the recurrence relations of Eqs. (22.16) and (22.17), while using $P = 5$ as the convergence parameter.

Step 8: Iterative analysis/redesign as described in Eqs. (22.16) and (22.17) while altering the mass of the damper is carried out until convergence to allowable levels. Upon convergence, TMDs with nonzero properties were located at frame number 1 (at floor 4), a sum of 10.69 ton added mass; at frame number 3 (at floor 8), a sum of 161.74 ton added mass, and at frame number 4 (at floor 8), a sum of 0.08 ton added mass which is the top floor for each part of the setback frame. At floor number 4, the TMDs are set to dampen mode 3 ($m = 10.69$ ton, $k = 1079.5$ kN/m, $\xi = 0.1045$), while at floor number 8, the TMDs are set to dampen modes 2 at frame 3 ($m = 161.74$ ton, $k = 5859.35$ kN/m, $\xi = 0.2137$) and at frame 4 ($m = 0.08$ ton, $k = 2.98$ kN/m, $\xi = 0.2137$). All three assigned TMDs add up to 9.68% of the original structure's mass. For all practical reasons, the small TMD at frame number 4 (at floor 8) can be neglected.

Finally, an analysis of the retrofitted structure yields the peripheral RMS accelerations shown in Fig. 22.6. As can be seen, only locations that had reached the maximum allowable RMS total acceleration (Fig. 22.6) were assigned with added absorbers, making the solution obtained a FSD.

22.5 Conclusions

An analysis/redesign performance-based methodology for optimally allocating and sizing MTMDs in 3D irregular structures was presented. The proposed methodology considers the possible dampening of all modes of the structure, at all peripheral frames, thus eliminating the decision of what modes to dampen and where the TMDs should be allocated. The methodology is general and automatically takes into consideration the structural irregularities; thus, no special attention has to be given to these complexities. As shown, using MTMDs tuned to various frequencies can efficiently reduce total accelerations within the structure and bring them to a desired level, allowing for performance-based design. The advantages of this methodology are its simplicity of use and relying solely on analysis tools to solve

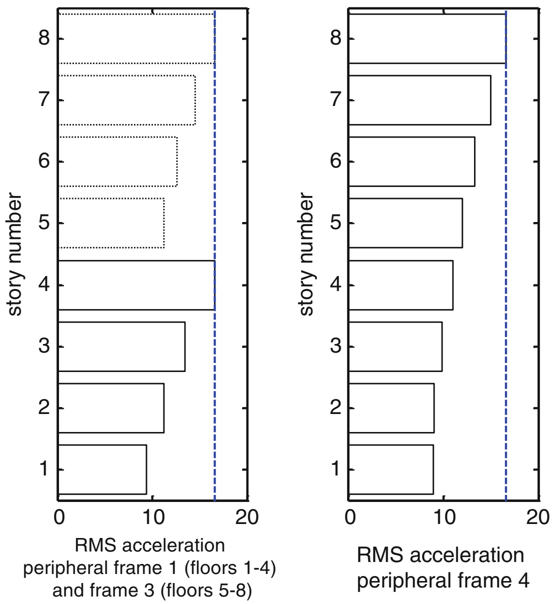

Fig. 22.6 Peripheral RMS accelerations of structure with final TMDs (*continuous* or *dotted*) and allowable values (*dashed*)

the allocation and sizing problem, with no assumptions or preselection of any design variable. These advantages make the proposed methodology attractive and efficient for practical use.

References

Abdel-Rohman M (1984) Optimal design of active TMD for buildings control. Build Environ 19(3):191–195

Ahlawat AS, Ramaswamy A (2003) Multiobjective optimal absorber system for torsionally coupled seismically excited structures. Eng Struct 25:941–950

Chen G, Wu J (2001) Optimal placement of multiple tune mass dampers for seismic structures. J Struct Eng 127(9):1054–1062

Christopoulos C, Filiatrault A (2006) Principles of supplemental damping and seismic isolation. IUSS Press, Milan

Cilley FH (1900) The exact design of statically indeterminate frameworks, an exposition of its possibility but futility. ASCE Trans 43:353–407

Clark AJ (1988) Multiple passive tuned mass dampers for reducing earthquake induced building motion. In: Proceedings of the 9th world conference on earthquake engineering, Tokyo-Kyoto, Japan, pp 779–784

Den-Hartog JP (1940) Mechanical vibrations, 2nd edn. McGraw-Hill Book Company Inc., New York

Desu NB, Dutta A, Deb SK (2007) Optimal assessment and location of tuned mass dampers for seismic control of a plan-asymmetrical buildings. Struct Eng Mech 26(4):459–477

Fu TS, Johnson EA (2011) Distributed mass damper system for integrating structural and environmental control in buildings. J Eng Mech. doi:10.1061/(ASCE)EM.1943-7889.0000211

Jangid RS, Datta TK (1997) Performance of multiple tuned mass dampers for torsionally coupled system. Earthq Eng Struct Dyn 20:307–317

Kanai K (1957) Semi-empirical formula for the seismic characteristics of the ground. Bull Earthq Res Ins Univ Tokyo 35:309–325

Kaynia AM, Veneziano D, Biggs JM (1981) Seismic effectiveness of tuned mass dampers. ASCE J Struct Div 107:1465–1484

Kwakernaak H, Sivan R (1991) Modern signals and systems. Prentice Hall, Englewood Cliffs

Lavan O, Levy R (2005) Optimal seismic retrofit of irregular 30 framed structures using supplemental viscous dampers. In: Proceedings of 4th European workshop on the seismic behaviour of irregular and complex structures, Thessaionica, Greece, paper no. 52, Aug 26–27

Levy R (1985) On the optimal design of trusses under one loading condition. Quart Appl Math 43(2):129–134

Levy R, Lavan O (2006) Fully stressed design of passive controllers in framed structures for seismic loadings. J Struct Multidis Optim 32:485–498

Li C, Qu W (2006) Optimum properties of multiple tuned mass dampers for reduction of translational and torsional response of structures subject to ground acceleration. Eng struct 28:472–494

Lin CC, Ueng JM, Huang EC (1999) Seismic response reduction of irregular buildings using passive tuned mass dampers. Eng struct 22:513–524

Lin CC, Wang JF, Lien CH, Chiang HW, Lin CS (2010) Optimum design and experimental study of multiple tuned mass dampers with limited stroke. Earth Eng Struct Dyn 39:1631–1651

Lin JL, Tsai KC, Yu YJ (2011) Bi-directional coupled tuned mass dampers for the seismic response control of two-way asymmetric-plan buildings. Earthq Eng Struct Dyn 40:675–690

Luo X, Ma R, Li G, Zhao D (2009) Parameter optimization of multi-mode vibration control system. In: International conference of measuring technology and mechatronics automation, IEEE Computer Society, pp 685–688

McNamara RJ (1977) Tuned mass dampers for buildings. ASCE J Struct Div 103:1785–1798

Mitchell AGM (1904) The limits of economy of Mateslal in framed structures. Philos Mag 6: 589–597

Moon KS (2010) Vertically distributed multiple tuned mass dampers in tall buildings: performance analysis and preliminary design. Struct Design Tall Spec Build 19:347–366

Nagarajaiah S, Sonmez E (2007) Structures with semiactive variable stiffness single/multiple tuned mass dampers. J Struct Eng 133(1):67–77

Newland DE (1993) An introduction to random vibrations, spectral & wavelet analysis. Prentice Hall, Harlow

Roffel AJ, Lourenco R, Narasimhan S (2010) Experimental studies on an adaptive tuned mass damper with real-time tuning capability. In: ASCE 19th analysis & computation specialty conference, 12–15 May 2010, pp 314–324

Singh MP, Singh S, Moreschi LM (2002) Tuned mass dampers for response control of torsional buildings. Earthq Eng Struct Dyn 31:749–769

Sladek JK, Klingner RE (1983) Effect of tuned-mass dampers on seismic response. ASCE J Struct Div 109:2004–2009

Somerville P, Smith N, Punyamurthula S, Sun J (1997) Development of ground motion time histories for phase 2 of the FEMA/SAC steel project. Report no. SAC/BD-97/04

Soong TT, Dargush GF (1997) *Passive* energy dissipation systems in structural engineering. Wiley, Chichester

Takewaki I (2009) Building control with passive dampers: optimal performance-based design for earthquakes. Wiley (Asia), Singapore

Tso WK, Yao S (1994) Seismic load distribution in buildings with eccentric setback. Can J Civil Eng 21:50–62

Warburton GB (1982) Optimum absorber parameters for various combinations of response and excitation parameters. Earthq Eng Struct Dyn 10:381–401

Xu K, Igusa T (1992) Dynamic characteristics of multiple substructures with closely spaced frequencies. Earthq Eng Struct Dyn 21:1059–1070